An Efficient Way of a Non-Hermitian Wavelet-based Signal Decomposition

BORIS M. SHUMILOV
Department of Applied Mathematics
Tomsk State University of Architecture and Building
2 Solyanaya, Tomsk, 634003
RUSSIA

Abstract: - The article investigates an implicit method of decomposition of the 7th degree non-Hermitian splines into a series of wavelets with two zero moments. The system of linear algebraic equations connecting the coefficients of the spline expansion on the initial scale with the spline coefficients and wavelet coefficients on the embedded scale is obtained. The even-odd splitting of the wavelet decomposition algorithm into a solution of the half-size five-diagonal system of linear equations and some local averaging formulas are substantiated. The results of numerical experiments on accuracy on polynomials and compression of spline-wavelet decomposition are presented.

Key-Words: - B-splines, wavelets, implicit decomposition relations, sweep method, data processing

Received: March 20, 2021. Revised: January 11, 2022. Accepted: February 5, 2022. Published: March 2, 2022.

1 Introduction

Laser scanning is a new direction in high-precision 3D measurements [1]. As to mobile scanning, scopes of application include positioning of the automobile and railroads, bridges, overpasses, city streets, the coastline, etc. The main advantage of laser scanning is the possibility to work at objects with heavy traffic, at industrial facilities without stopping production and in hard-to-reach sites, and also at objects having a complex configuration [2]. As the principle of a mobile scanning system allows working on the road without traffic overlapping, the cloud of data points from laser scanning devices contains a roadside landscape and hindrances on the carriageway (reflection from people who are on the object, technique, vegetation, etc.). The main goals of preliminary processing of laser scanned data are removal of a roadside and surrounding landscape, filling of gaps in the scanned data, created by cars passing by on the carriageway, and the elaboration of the planned axial line of the road [3]. From the mathematical point of view, the production of the axis of the road allows transforming bends of the highway to some rectangular area, for which it is possible to apply standard methods of two-dimensional spline interpolation [4] on a rectangular grid, keeping structural lines of the road (edges, brows), unlike the popular method of restoration of a surface of the highway by triangulation of chaotic points [5]. Very important is that at such approach high precision of detection of cracks and damages of road pavement in the places demanding repair is guaranteed and construction and application of wavelet-transformation of interpolation splines for compression of the scanned information in the places of highways not demanding repair are significantly facilitated also. Cubic splines of smoothness of C^2 became popular for road engineers as an adequate way of mathematical representation of picket method of tracing of the reconstructing highways. As for Hermite splines they allow in an explicit form, using the values of spline coefficients, to consider geometrical restrictions on control points (pickets of the automobile route), and on route tangents (the directions of tangent lines at the entrance on bridge construction or at adjunction) and radiuses of transition curves (values of curvature on accelerating and brake sections of the route).

In the theory of a multi-scale analysis, the basis of the space that fills the difference between approximating spaces on a dense grid and a thinned grid are called wavelets [6, p. 41]. Unlike Fourier transform, which provides only amplitude-frequency information but loses time information, discrete wavelet transform analyses the signal in a time-frequency domain [6-9]. For example, effective denoising methods are required for processing measured signals, because conventional denoising methods may not be practical due to the noisy nature of the measuring as well as its spectral overlap with different noise sources [10, 11]. The unique properties of wavelets allow designing a basis in which the data representation can be expressed with a small number of non-zero coefficients. This property makes wavelets attractive for data compression, including video and audio information. Wavelet transform can be viewed as one of the methods of primary signal processing to improve the efficiency of its compression. In this case, direct compression is performed by classical methods only for significant coefficients of the wavelet decomposition of the signal, and its reconstruction according to these coefficients is performed at the stage of restoration (decompression) [12]. With multimedia becoming widely popular, the conflict between massive data and finite memory devices has been continuously intensified; so, it requires more convenient, efficient, and high-quality transmission and storage technology, and the fast wavelet analysis is what people want to use for highly efficient compression technology [13-16].

The Haar wavelets and Daubechies wavelets were the first orthonormal wavelets with compact supports [6]. Their generalizations were constructed by Cohen et al in the form of biorthogonal wavelets [17, 18]. The compactness means that there exist explicit finite formulas for the discrete wavelet decomposition. But the disadvantage of these wavelets is that the expansion coefficients are calculated using local averaging formulas, that is, the information at the edges of the image is lost during data processing [19]. For the indicated problem of roads construction, it is important to complement smoothly the discretely given functions. Not all types of wavelets meet these goals, but only some of them, for example, wavelets based on B-splines and Hermitian splines [20].

Usually, the construction of basis functions in the wavelet space begins with the use of basis functions in the approximating space with centers at odd nodes of a dense grid (”lazy” wavelets [8]). We proposed to use approximating basis functions with centers at even nodes [21, 22] as ”lazy” wavelets. Since the wavelet space must be the complement of the approximating spaces on dense and thinned grids, the dimensions of these spaces must satisfy the so-called dimension relation. Sometimes, to fulfill this condition, it is sufficient to restrict ourselves to considering the periodic case when the values of the coefficients at the ends of the approximation segment coincide. This corresponds to the approximation of closed curves and surfaces. For open curves, a mismatch occurs. So we considered previously unknown types of Hermitian wavelets of the third [21] and seventh [22] degrees, proved the existence of finite implicit expansion relations, and substantiated effective algorithms for wavelet analysis based on them. Namely, for the case of the third degree, we proposed to subtract from the initial coordinates the equation of the straight line connecting the first and last points. Then the two basis functions along the edges of the segment are removed from the bases, and the dimensions of the resulting spaces provide the dimension relation. For the case of the seventh degree, a variant was investigated in detail that leads to the most compact solution when the equation of a cubic parabola interpolating the function and the second derivative at the first and last points is subtracted from the initial coordinates. As a result, the corresponding basis functions are removed from the bases, and the dimension relation is also fulfilled. For the cases of the first and fifth degrees, such symmetric solutions do not exist.

Wavelet transforms based on Hermite splines have their drawbacks. First, in the problem of processing measurement information, one must calculate the approximate values of the derivatives at the nodes of the densest grid with acceptable accuracy [23], and only then can wavelet transform algorithms be applied. Secondly, from the point of view of data compression, the number of wavelet coefficients, in this case, is greater than in methods based on B-splines. Meanwhile, in the work of the author [24], non-orthogonal wavelets of the third degree with the first six zero moments, that is, orthogonal to all polynomials of the five-degree, were considered; the existence of finite implicit decomposition relations was proved, and an effective algorithm for wavelet analysis based on them was justified. The importance of the new algorithm in wavelets theory is its stability and the simplicity of realization because a matrix possessing strict diagonal prevalence is solved at each step of resolution.

This article is a first attempt to find out if there is an even-odd splitting algorithm for non-orthogonal wavelets of the seventh degree with the two first zero moments. Section 2 discusses the properties of the splines of degree m of smoothness C^{m-1} on a uniform infinite grid of nodes and the non-orthogonal spline-wavelets with $n+1$ vanishing moments. Section 3 considers the use of the matrix notation to wavelet transformation of hierarchical spline bases and suggests the main idea of preconditioning the wavelet transform system of equations. As a result, in section 4 the case of spline-wavelets of seventh-degree with 2 zero moments is fully resolved and in section 5 the wavelet interpolation algorithm on the finite segment is implemented. In the sixth section, the algorithm of wavelet analysis is presented as a whole, and section 7 contains an example of the application.

2 Construction of spline wavelets with vanishing moments

The basis for constructing wavelets is the presence of a set of approximating spaces $\ldots V_{L-1} \subset V_L \subset V_{L+1} \ldots$ such that each basis function in V_L can be expressed as a linear combination of basis functions in

V_{L+1}. In particular, splines – smooth functions glued from pieces of polynomials of degree m on an embedded sequence of grids, have this property. The essence of the wavelet transform can be formulated as follows: it allows one to decompose a given function V_{L+1} into a rough approximate representation V_L and local refinements $W_L = V_{L+1} - V_L$. The procedure for dividing into a rough version and clarifying details can be applied recursively to this part of V_L. Hence, the original function can be represented as a hierarchy of rough versions of $V_L, V_{L-1}, ...$ and refinements $W_L, W_{L-1}, ...$ Such a recursive process is called direct wavelet transformation (decomposition or analysis) [9, p. 46]. Conversely, the function V_{L+1} can be reconstructed from the most compact representation (reconstruction). Moreover, the values of the coefficients of the wavelet decomposition can be used to judge the significance of the corresponding details of the refinement. Insignificant details can be removed to compress the information. The main thing here is to find a suitable basis for the space W_L and construct for it fast one-to-one formulas for the direct and inverse wavelet transforms.

Let the space V_L be the space of splines of degree m of smoothness C^{m-1} on a uniform grid of nodes $\Delta^L : x_{i+1} = x_i + 1/2^L$, infinitely extended in both directions for all i. It is well known that the basis in this space is generated by functions $\varphi_m(v - i)\forall i$, where $v = 2^L x$, generated by contractions and shifts of a function of the form [9, p. 89]:

$$\varphi_m(t) = \frac{1}{m!}\sum_{j=0}^{m+1}(-1)^j\binom{m+1}{j}(t-j)_+^m,$$

where $t_+^m = (\max\{t, 0\})^m$.

They have the following supports,

$$\operatorname{supp}\varphi_m = [0, m+1],$$

and they satisfy the calibration relation [9, p. 91]:

$$\varphi_m(t) = 2^{-m}\sum_{k=0}^{m+1}\binom{m+1}{k}\varphi_m(2t-k). \quad (1)$$

As a result, any spline on the mesh Δ^L can be represented as

$$s^L(x) = \sum_{-\infty}^{\infty} c_i^L \varphi_m(2^L x - i), \quad (2)$$

where the coefficients $c_i^L\forall i$ are the solution, for example, of the cardinal interpolation problem:

$$s^L(x_i) = f(x_i),\ -\infty < i < \infty.$$

If the grid Δ^{L-1} is obtained from the grid Δ^L by removing every second node, then the corresponding space V_{L-1} with basic functions $\varphi_m(v/2 - i)\forall i$, whose supports are twice as wide in width, is embedded in V_L. The difference between the spaces V_L and V_{L-1} constitutes the wavelet space $W_{L-1} = V_L - V_{L-1}$ [9].

In what follows we will use non-orthogonal wavelets with $n+1$ vanishing moments, that is, orthogonal to all polynomials of degree n [25],

$$w_{m,n}(t) = 2^{-m}\sum_{k=0}^{n+1}(-1)^k\binom{n+1}{k}\varphi_m(2t-k). \quad (3)$$

These functions have the following supports

$$\operatorname{supp} w_{m,n} = [0, \frac{m+n}{2} + 1]$$

and, accordingly, $n+1$ zero moments

$$\int_{-\infty}^{\infty} x^k w_{m,n}(x)dx = 0,\ k = 0, 1, \ldots, n.$$

For the case, $m = 7$, the basis spline function takes on a form (Fig. 1).

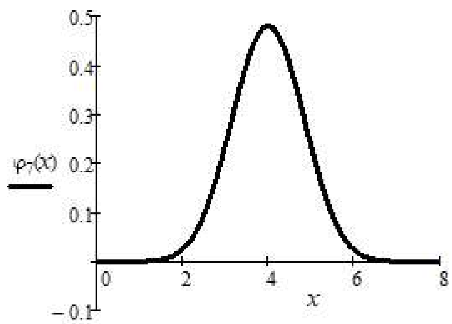

Figure 1: The graph of the scaling function $\varphi_7(x)$

The graph of wavelet of the 7th degree, orthogonal to all polynomials of the 1st degree, is shown in figure 2.

3 Construction of the defining system of wavelet transform equations

We write the basic spline functions in the form of a one-row matrix of infinite length,

$$\varphi^L(x) = \\ = \left[\ldots, \varphi_m(2^L x - i), \varphi_m(2^L x - i - 1), \ldots\right].$$

Introducing the notation

$$\mathbf{c}^L = \left[\ldots, c_i^L, c_{i+1}^L, \ldots\right]^T$$

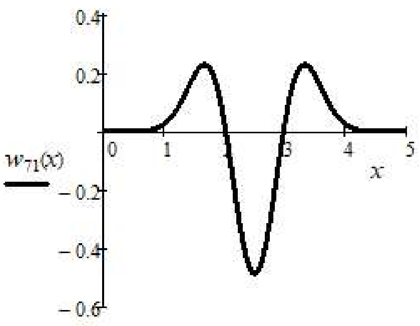

Figure 2: The graph of the function $128 \cdot w_{7,1}(x)$

for a vector consisting of the spline coefficients, we write the formula (2) in a vector form

$$s^L(x) = \varphi^L(x)\mathbf{c}^L.$$

In the same way, we can write basic wavelet functions at the decomposition level L in the form of an infinite row matrix as

$$\psi^{L-1}(x) = \\ = \left[\ldots, w_{m,n}(2^L x - i), w_{m,n}(2^L x - i - 1), \ldots\right].$$

We denote the corresponding wavelet approximation coefficients by $d_i^{L-1}, -\infty < i < \infty$, and introduce the column vector

$$\mathbf{d}^{L-1} = \left[\ldots, d_i^{L-1}, d_{i+1}^{L-1}, \ldots\right]^T.$$

Since the spaces V_{L-1} and W_{L-1} are by definition subspaces of V_L, the functions $\varphi^{L-1}(x)$ and $\psi^{L-1}(x)$ can be represented as linear combinations of the functions $\varphi^L(x)$:

$$\begin{array}{rcl} \varphi^{L-1}(x) & = & \varphi^L(x)P^L, \\ \psi^{L-1}(x) & = & \varphi^L(x)Q^L, \end{array}$$

where the columns of the matrix P^L are composed of the relation coefficients (1) since each wide basic function can be constructed from $m+2$ narrow basic functions, while the elements of the columns of the matrix Q^L are composed of the relation coefficients (3).

Therefore, there is a chain of equalities:

$$\begin{array}{rl} \varphi^L(x)\mathbf{c}^L = & \varphi^{L-1}(x)\mathbf{c}^{L-1} + \psi^{L-1}(x)\mathbf{d}^{L-1} = \\ = & \varphi^L(x)P^L\mathbf{c}^{L-1} + \varphi^L(x)Q^L\mathbf{d}^{L-1}. \end{array}$$

Let the coefficients $\mathbf{c}^{L-1}$ and $\mathbf{d}^{L-1}$ be known. Then the coefficients $\mathbf{c}^L$ can be easily obtained from $\mathbf{c}^{L-1}$ and $\mathbf{d}^{L-1}$ as follows

$$\mathbf{c}^L = P^L\mathbf{c}^{L-1} + Q^L\mathbf{d}^{L-1}. \tag{4}$$

Using the notation for block matrices, we can rewrite equality (4) in the form

$$\mathbf{c}^L = \left[P^L \mid Q^L\right] \left[\frac{\mathbf{c}^{L-1}}{\mathbf{d}^{L-1}}\right]. \tag{5}$$

Formula (5) is nothing more than a recovery algorithm [9, p. 248], for the implementation of which, due to tape matrices P^L and Q^L the moving average scheme is successfully used. For example, for the case $m = 7,\ n = 1$, the infinite matrix $\left[P^L \mid Q^L\right]$ takes the following form:

$$\left[P^L \mid Q^L\right] = \frac{1}{128}\cdot$$

$$\cdot \left[\begin{array}{cccc|cccc}
 & \vdots & & & & & & \\
\ddots & 0 & & & & & & \\
\ddots & 1 & \vdots & & & & & \\
\ddots & 8 & 0 & & & & & \\
\ddots & 28 & 1 & \ddots & & \vdots & & \\
\ddots & 56 & 8 & \ddots & \ddots & 0 & & \\
\ddots & 70 & 28 & \ddots & \ddots & 1 & \vdots & \\
\ddots & 56 & 56 & \ddots & \ddots & -2 & 0 & \ddots \\
\ddots & 28 & 70 & \ddots & \ddots & 1 & 1 & \ddots \\
\ddots & 8 & 56 & \ddots & \ddots & 0 & -2 & \ddots \\
\ddots & 1 & 28 & \ddots & & \vdots & 1 & \ddots \\
\ddots & 0 & 8 & \ddots & & & 0 & \ddots \\
 & \vdots & 1 & \ddots & & & \vdots & \\
 & & 0 & \ddots & & & & \\
 & & \vdots & & & & &
\end{array}\right].$$

Unfortunately, for the reverse process of calculating from the coefficients $\mathbf{c}^L$ the coarser version $\mathbf{c}^{L-1}$ and the refining coefficients $\mathbf{d}^{L-1}$, following the decomposition algorithm [9, p. 247]

$$\left[\frac{\mathbf{c}^{L-1}}{\mathbf{d}^{L-1}}\right] = \left[\frac{A^L}{B^L}\right]\mathbf{c}^L,$$

we obtain for all cases, except for the case of the Haar wavelets, that the rows of matrices A^L and B^L are infinite numerical sequences, and their truncation leads to errors.

4 The algorithm with splitting

As can be seen from the above example, the resulting system of equations has some sort of a step-wise structure, which permits the application of the method of even-odd splitting to the system solving [24]. We choose for this purpose some preconditioning matrix R^L to receive the easy invertible matrix

$$G^L = \left[P^L \mid Q^L\right] R^L$$

by the conditions:
a) a matrix G^L is a tape matrix with the minimum possible number of nonzero diagonals;
b) R^L is a tape matrix, with the minimum possible number of elements.

By placing as many zeros as possible in the upper and lower parts of each column of the matrix R^L, we ensure the compactness of the computational scheme; by zeroing the elements spaced by an odd number of steps from the main diagonal of the matrix G^L, we provide the possibility of using an efficient sweep method for solving it; and additionally zeroing the elements outside the main diagonal of the matrix G^L, we provide the possibility of the subsequent splitting of the system into even and odd rows.

Then, assuming that the matrix G^L is nondegenerate, we multiply the left and right sides of equality (5) by the matrix $R^L G^{L^{-1}}$. As a result, we get

$$\begin{aligned} &R^L G^{L^{-1}} \mathbf{c}^L = \\ &= R^L \left(\left[P^L \mid Q^L\right] R^L\right)^{-1} \left[P^L \mid Q^L\right] \left[\frac{\mathbf{c}^{L-1}}{\mathbf{d}^{L-1}}\right] = \\ &= R^L R^{L^{-1}} \left[\frac{A^L}{B^L}\right] \left[P^L \mid Q^L\right] \left[\frac{\mathbf{c}^{L-1}}{\mathbf{d}^{L-1}}\right] = \\ &= \left[\frac{\mathbf{c}^{L-1}}{\mathbf{d}^{L-1}}\right]. \end{aligned}$$

Thus, instead of directly solving a system of the form (5), we can solve the system

$$G^L \mathbf{h}^L = \mathbf{c}^L \tag{6}$$

with respect to some values of $\mathbf{h}^L$ and then just calculate the values of $\mathbf{c}^{L-1}$ and $\mathbf{d}^{L-1}$ using the linear transformation

$$\left[\frac{\mathbf{c}^{L-1}}{\mathbf{d}^{L-1}}\right] = R^L \mathbf{h}^L. \tag{7}$$

For the matrix, $\left[P^L \mid Q^L\right]$, the nine-diagonal matrix

$$\left[P^L \mid Q^L\right]' = \frac{1}{128} \cdot \begin{bmatrix} \ddots & \vdots & \vdots & & & & & & \\ \ddots & 0 & 0 & \vdots & & & & & \\ \ddots & 0 & 1 & 0 & \vdots & & & & \\ \ddots & 0 & 8 & 0 & 0 & \vdots & & & \\ \ddots & 1 & 28 & 0 & 1 & 0 & \ddots & & \\ \ddots & -2 & 56 & 0 & 8 & 0 & 0 & \cdots & \\ \ddots & 1 & 70 & 1 & 28 & 0 & 1 & 0 & \cdots \\ \ddots & 0 & 56 & -2 & 56 & 0 & 8 & 0 & \cdots \\ \ddots & 0 & 28 & 1 & 70 & 1 & 28 & 0 & \ddots \\ \cdots & 0 & 8 & 0 & 56 & -2 & 56 & 0 & \ddots \\ \cdots & 0 & 1 & 0 & 28 & 1 & 70 & 1 & \ddots \\ & \ddots & 0 & 0 & 8 & 0 & 56 & -2 & \ddots \\ & & \vdots & 0 & 1 & 0 & 28 & 1 & \ddots \\ & & & \vdots & 0 & 0 & 8 & 0 & \ddots \\ & & & & \vdots & \vdots & \ddots & \ddots & \ddots \end{bmatrix}$$

is obtained by permuting the columns of the matrix $\left[P^L \mid Q^L\right]$ so that the columns of the matrices P^L and Q^L alternate. In practice, such a permutation is accompanied by a change in the order of the unknowns in the system (5) and is often done to give the system a tape-like form to facilitate the numerical solution of the system [8]. Let the matrix corresponding to the indicated permutation of columns is denoted by T. Then the representation is true [26]

$$\left[P^L \mid Q^L\right]' = \left[P^L \mid Q^L\right] T. \tag{8}$$

From the representation (8) we find

$$\left[P^L \mid Q^L\right]^{-1} \cdot G^L = T \cdot \left[P^L \mid Q^L\right]'^{-1} \cdot G^L. \tag{9}$$

Thus, the problem of finding the matrices R^L and G^L is reduced to finding a solution of the system of matrix equalities

$$\left[P^L \mid Q^L\right]'_j R^{L'}_j = G^L_j, \ -\infty < j < \infty. \tag{10}$$

Here, the subscripts in the notation of the matrices indicate which elements of the columns of the matrix $R^{L'}$ are calculated by the corresponding system (10). Specifically, according to the assumed stepped structure of the matrices $R^{L'}$ and G^L, system (10) splits into blocks with matrices of the following form:

$$\left[P^L \mid Q^L\right]'_{j,j+1,\dots,j+6} = \frac{1}{128} \cdot$$

$$\cdot\begin{bmatrix} 1 & 28 & 0 & 1 & & & & & \\ -2 & 56 & 0 & 8 & & & & & \\ 1 & 70 & 1 & 28 & 0 & 1 & & & \\ 0 & 56 & -2 & 56 & 0 & 8 & & & \\ 0 & 28 & 1 & 70 & 1 & 28 & & & \\ 0 & 8 & 0 & 56 & -2 & 56 & & & \\ & 1 & 0 & 28 & 1 & 70 & 1 & & \\ & 0 & 0 & 8 & 0 & 56 & -2 & & \\ & & 0 & 1 & 0 & 28 & 1 & & \end{bmatrix},$$

provided that the equations corresponding to the zero rows of the matrix G^L are removed from the system. This system is solvable and underdetermined. Therefore, we can choose non-trivial solutions that interest us, namely:

$$\begin{aligned} 1)\quad & r_0 = r_6 = 4;\ r_1 = r_5 = 0; \\ & r_2 = r_4 = 28;\ r_3 = 1; \\ & g_0 = g_8 = 5; \\ & g_1 = g_3 = g_5 = g_7 = 0; \\ & g_2 = g_6 = 60;\ g_4 = 126; \\ 2)\quad & r_0 = r_1 = r_3 = r_4 = r_5 = r_6 = 0; \\ & r_2 = 1; \\ & g_0 = g_1 = g_5 = g_6 = g_7 = g_8 = 0; \\ & g_2 = g_4 = 1;\ g_3 = -2; \\ 3)\quad & r_0 = r_1 = r_2 = r_3 = r_5 = r_6 = 0; \\ & r_4 = 1; \\ & g_0 = g_1 = g_2 = g_3 = g_7 = g_8 = 0; \\ & g_4 = g_6 = 1;\ g_5 = -2. \end{aligned}$$

As a result, the matrix G^L acquires a tape structure with seven nonzero diagonals of the form

$$\begin{bmatrix} \ddots & \ddots & \ddots & & & & & \\ \ddots & 0 & 5 & \ddots & & & & \\ \ddots & 0 & 0 & 0 & \ddots & & & \\ \ddots & 1 & 60 & 0 & 5 & \ddots & & \\ \ddots & -2 & 0 & 0 & 0 & \ddots & & \\ \ddots & 1 & 126 & 1 & 60 & 0 & \ddots & \\ \ddots & 0 & 0 & -2 & 0 & 0 & \ddots & \\ \ddots & 0 & 60 & 1 & 126 & 1 & \ddots & \\ \ddots & 0 & 0 & 0 & 0 & -2 & \ddots & \\ \ddots & 0 & 5 & 0 & 60 & 1 & \ddots & \\ & \ddots & 0 & 0 & 0 & 0 & \ddots & \\ & & \ddots & 0 & 5 & 0 & \ddots & \\ & & & \ddots & 0 & 0 & \ddots & \\ & & & & \ddots & \ddots & \ddots & \end{bmatrix},$$

while the product of matrices $\left[P^L \mid Q^L\right]'^{-1} \cdot G^L$ turns out to have the following form:

$$\begin{bmatrix} \ddots & \ddots & \ddots & & & & & \\ \ddots & 0 & 0 & \ddots & & & & \\ \ddots & 0 & 4 & 0 & \ddots & & & \\ \ddots & 0 & 0 & 0 & 0 & \ddots & & \\ \ddots & 1 & 28 & 0 & 4 & 0 & \ddots & \\ \ddots & 0 & 1 & 0 & 0 & 0 & \ddots & \\ \ddots & 0 & 28 & 1 & 28 & 0 & \ddots & \\ \ddots & 0 & 0 & 0 & 1 & 0 & \ddots & \\ \ddots & 0 & 4 & 0 & 28 & 1 & \ddots & \\ & \ddots & 0 & 0 & 0 & 0 & \ddots & \\ & & \ddots & 0 & 4 & 0 & \ddots & \\ & & & \ddots & 0 & 0 & \ddots & \\ & & & & \ddots & \ddots & \ddots & \end{bmatrix}. \tag{11}$$

From equality (8) it follows that to find the matrix $R^L = \left[P^L \mid Q^L\right]^{-1} \cdot G^L$, it is required to apply to the rows of the matrix (11) an inverse permutation, that is, a permutation in which the records of the image and the inverse image are interchanged. From this, we can obtain the required in (7) representation of the matrix R^L.

5 The case of a finite segment

Recall that for the case of interpolation by splines on a finite interval $[0, 2^L]$, the most productive approach to constructing basis functions is to set multiple nodes at the ends of the interval, which corresponds to zeroing of the approximating spline and some of its derivatives at the ends of the interval [8]. Then the left basic functions have the view forms (Fig. 3, Fig. 4).

They have the following supports,

$$\operatorname{supp}\varphi_{b1} = [0,7],\ \operatorname{supp}\varphi_{b2} = [0,6],$$

and they satisfy the calibration relations

$$\begin{aligned} \varphi_{b1}(t) = {} & \frac{1}{64}\varphi_{b1}(2t) + \frac{19}{134}\varphi_7(2t) + \\ & + \frac{59}{160}\varphi_7(2t-1) + \frac{327}{640}\varphi_7(2t-2) + \\ & + \frac{41}{96}\varphi_7(2t-3) + \frac{167}{768}\varphi_7(2t-4) + \\ & + \frac{1}{16}\varphi_7(2t-5) + \frac{1}{128}\varphi_7(2t-6), \\ \varphi_{b2}(t) = {} & \frac{1}{32}\varphi_{b2}(2t) + \frac{147}{640}\varphi_{b1}(2t) + \frac{12299}{25600}\varphi_3(2t) + \end{aligned}$$

$$+\frac{371}{800}\varphi_7(2t-1)+\frac{399}{1600}\varphi_7(2t-2)+$$
$$+\frac{7}{96}\varphi_7(2t-3)+\frac{7}{768}\varphi_7(2t-4).$$

As to boundary basic wavelets, we use the wavelets of seventh-degree that are orthogonal to all first-degree polynomials (Fig. 5, Fig. 6),

$$w_{b1}(t)=\frac{7}{48}\varphi_{b2}(2t)-\frac{15}{64}\varphi_{b1}(2t)+\frac{49}{512}\varphi_7(2t),$$
$$w_{b2}(t)=\frac{1}{16}\varphi_{b2}(2t)-\frac{11}{128}\varphi_7(2t)+\frac{5}{128}\varphi_7(2t-2).$$

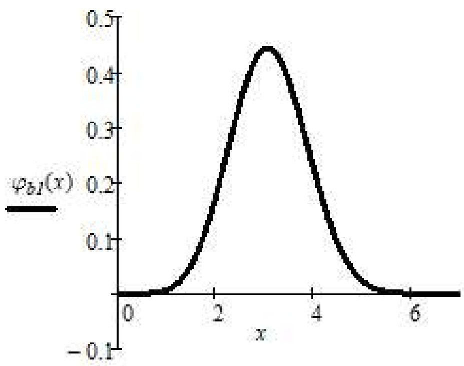

Figure 3: The graph of the scaling function $\varphi_{b1}(x)$

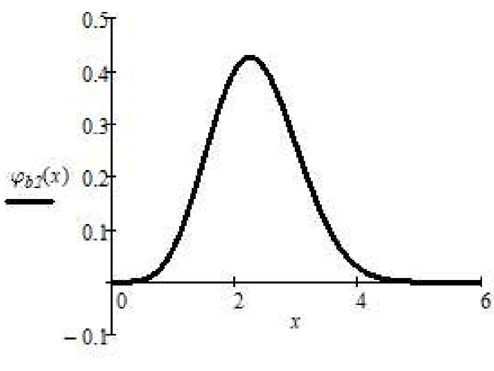

Figure 4: The graph of the scaling function $\varphi_{b2}(x)$

They have the following supports

$$\operatorname{supp} w_{b1}=[0,5],\ \operatorname{supp} w_{b2}=[0,4],$$

and, accordingly, they have two zero moments

$$\int_0^5 x^k w_{b1}(x)dx=\int_0^4 x^k w_{b2}(x)dx=0,$$

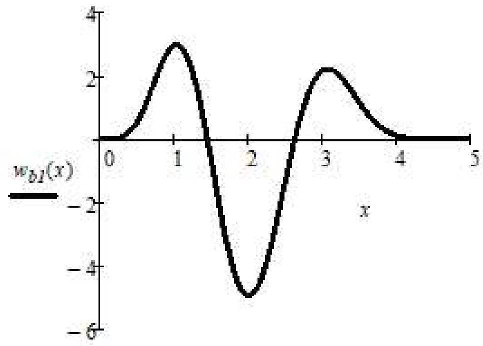

Figure 5: The graph of the function $128\cdot w_{b1}(x)$

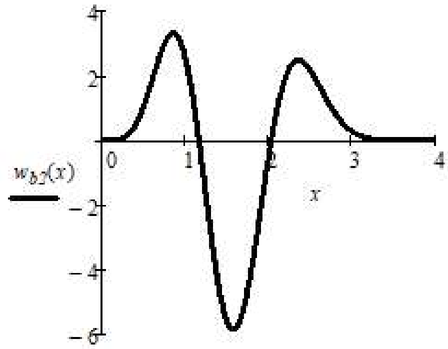

Figure 6: The graph of the function $128\cdot w_{b2}(x)$

for $k=0,1$.

At the right end of the segment, the basic functions mirror the functions $\varphi_{b1,2}(t), w_{b1,2}(t)$. As a result, for any grid Δ^L, $L\geq 3$, a seven-degree spline with zero boundary conditions

$$\left(s^L\right)^{(r)}(v)=0,\ r=0,1,2,3,\ v=0,2^L,$$

can be represented as

$$s^L(v)=c^L_{-2}\varphi_{b2}(v)+c^L_{-1}\varphi_{b1}(v)+$$
$$+\sum_{i=0}^{2^L-8}c_i^L\varphi_7(v-i)+c^L_{2^L-3}\varphi_{b1}(2^L-v)+$$
$$+c^L_{2^L-2}\varphi_{b2}(2^L-v), 0\leq v\leq 2^L,$$

where the coefficients $c_i^L\forall i$ are the solution, for example, of the interpolation problem:

$$s^L(i)\ \ =\ \ f(i),\ i=2,3,\ldots,2^L-2.$$

To prepare the system (5) for the odd-even splitting we need to solve the system (11) for indices $j = -2, -1, \ldots, 5$ with the following matrix

$$\left[P^L \mid Q^L\right]'_{-2,-1,\ldots,5} = \frac{1}{128}\cdot$$

$$\cdot\begin{bmatrix} 8 & \frac{56}{3} & 4 & 0 & & & & \\ 0 & -30 & \frac{147}{5} & 0 & 2 & & & \\ -11 & \frac{49}{4} & \frac{12299}{200} & 1 & \frac{1216}{67} & 0 & 1 & \\ 0 & 0 & \frac{1484}{25} & -2 & \frac{236}{5} & 0 & 8 & \\ 5 & 0 & \frac{798}{25} & 1 & \frac{327}{5} & 1 & 28 & 0 \\ 0 & 0 & \frac{28}{3} & 0 & \frac{164}{3} & -2 & 56 & 0 \\ & 0 & \frac{7}{6} & 0 & \frac{167}{6} & 1 & 70 & 1 \\ & & 0 & 0 & 8 & 0 & 56 & -2 \\ & & & 0 & 1 & 0 & 28 & 1 \end{bmatrix},$$

provided that the equations corresponding to the zero rows of the matrix G^L are removed from the system. This system is solvable and underdetermined. Therefore, we can choose any non-trivial solutions that interest us, for example:

1) $$r_{-2} = 1;$$
$$r_{-1} = r_0 = r_1 = r_2 = r_3 = r_4 = r_5 = 0;$$
$$g_{-2} = 8;\; g_{-1} = g_1 = g_3 = g_4 = g_5 = 0;$$
$$g_0 = -11;\; g_2 = 5;$$

2) $$r_{-2} = r_0 = r_1 = r_2 = r_3 = r_4 = r_5 = 0;$$
$$r_{-1} = 1;$$
$$g_{-2} = \tfrac{56}{3};\; g_{-1} = -30;\; g_0 = \tfrac{49}{4};$$
$$g_1 = g_2 = g_3 = g_4 = g_5 = 0;$$

3) $$r_{-2} = -\tfrac{418}{25};\; r_{-1} = \tfrac{147}{25};$$
$$r_0 = 6;\; r_1 = \tfrac{4452}{25};$$
$$r_2 = r_4 = r_5 = r_6 = r_7 = r_8 = 0;$$
$$r_3 = 28;$$
$$g_{-2} = g_{-1} = g_1 = g_3 = g_5 =$$
$$= g_7 = g_8 = g_9 = g_{10} = g_{11} = 0;$$
$$g_0 = 803;\; g_2 = 314;\; g_4 = 35;$$

4) $$r_{-2} = r_{-1} = r_0 = r_2 = r_3 = r_4 = r_5 = 0;$$
$$r_1 = 1;$$
$$g_{-2} = g_{-1} = g_4 = g_5 = 0;$$
$$g_0 = g_2 = 1;\; g_1 = -2;$$

5) $$r_{-2} = -\tfrac{78973}{7875};\; r_{-1} = \tfrac{1327}{375};$$
$$r_0 = \tfrac{124}{35};\; r_1 = \tfrac{16094}{125};\; r_2 = 1;$$
$$r_3 = \tfrac{658}{15};\; r_5 = 4;$$
$$r_4 = r_6 = r_7 = r_8 = 0;$$
$$g_{-2} = g_{-1} = g_1 = g_3 = g_5 = g_7 =$$
$$= g_8 = g_9 = g_{10} = g_{11} = 0;$$
$$g_0 = \tfrac{43765811}{84420};\; g_2 = \tfrac{94804}{315};$$
$$g_4 = \tfrac{479}{6};\; g_6 = 5;$$

6) $$r_{-2} = r_{-1} = r_0 =$$
$$r_1 = r_2 = r_4 = r_5 =$$
$$= r_6 = r_7 = r_8 = 0;$$
$$r_3 = 1;$$
$$g_{-2} = g_{-1} = g_0 = g_6 =$$
$$= g_7 = g_8 = g_9 = g_{10} = g_{11} = 0;$$
$$g_2 = g_4 = 1;\; g_3 = -2.$$

So, the first seven columns of the matrix G^L are

$$\begin{bmatrix} 8 & \frac{56}{3} & 0 & 0 & 0 & 0 & 0 \\ 0 & -30 & 0 & 0 & 0 & 0 & 0 \\ -11 & \frac{49}{4} & 803 & 1 & \frac{43765811}{84420} & 0 & 5 \\ 0 & 0 & 0 & -2 & 0 & 0 & 0 \\ 5 & 0 & 314 & 1 & \frac{94804}{315} & 1 & 60 \\ 0 & 0 & 0 & 0 & 0 & -2 & 0 \\ 0 & 0 & 35 & 0 & \frac{479}{6} & 1 & 126 \\ 0 & 0 & 0 & 0 & 0 & 0 & 0 \\ 0 & 0 & 0 & 0 & 5 & 0 & 60 \\ 0 & 0 & 0 & 0 & 0 & 0 & 0 \\ 0 & 0 & 0 & 0 & 0 & 0 & 5 \\ \vdots & \vdots & \vdots & \vdots & \vdots & \vdots & \vdots \end{bmatrix}.$$

From the structure of the matrix G^L it immediately follows, that the values of $\mathbf{h}^L$ at odd nodes are calculated from the explicit equations

$$\frac{c_i^L}{h_i} = \begin{cases} 30, & i = \quad -1,, 2^L - 3; \\ 2, & i = \quad 1, 3, \ldots, 2^L - 5, \end{cases},$$

while for the values of $\mathbf{h}^L$ at even nodes a system of linear equations is solved:

$$\begin{aligned} 8h_{-2} &= r_{-2}, \\ -11h_{-2} + 803h_0 + \frac{43765811}{84420}h_2 + 5h_4 &= r_0, \\ 5h_{-2} + 314h_0 + \frac{94804}{315}h_2 + 60h_4 + 5h_6 &= r_2, \end{aligned}$$

$$
\begin{aligned}
35h_0+\frac{479}{6}h_2+126h_4+60h_6+5h_8 &= r_4,\\
\left.\begin{array}{r}
i=6,8,\dots,2^L-10:\\
5h_{i-4}+60h_{i-2}+126h_i+60h_{i+2}+5h_{i+4}\\
i=2^L-8:\\
5h_{i-4}+60h_{i-2}+126h_i+\frac{479}{6}h_{i+2}+35h_{i+6}\\
i=2^L-6:\\
5h_{i-4}+60h_{i-2}+\frac{94804}{315}h_i+314h_{i+2}+5h_{i+4}\\
i=2^L-4:\\
5h_{i-6}+\frac{43765811}{84420}h_{i-4}+803h_i-11h_{i+2}\\
i=2^L-2:\\
8h_i
\end{array}\right\} &= r_i.
\end{aligned}
\tag{12}
$$

Here the right-hand sides of the equations (12) are calculated from the formulas

$$
\begin{aligned}
r_{-2} &= c^L_{-2}+\frac{56}{3}h_{-1},\\
r_0 &= c^L_0+\frac{49}{4}h_{-1}+h_1,\\
r_i &= \begin{cases}
c^L_i+h_{i-1}+h_{i+1}, \\
i=2,4,\dots,2^L-6,\\
c^L_i+h_{i-1}+\frac{49}{4}h_{i+1},\\
i=2^L-4,\\
c^L_i+\frac{56}{3}h_{i-1},\\
i=2^L-2.
\end{cases}
\end{aligned}
$$

Note that the matrix of the system (12) has not a strict diagonal dominance [27, p. 78] over the columns of the system. So, although the system of equations has a unique solution because of linear independence of basis functions, the stability of the calculations by the sweep method is not guaranteed.

Multiplying the matrices $\left[P^L \mid Q^L\right]^{-1}$ and G^L we can recheck the analytical evaluation provided to obtain that the matrix R^L is composed of two blocks according to $2^{L-1}-3$ basic spline functions of V_{L-1} and 2^{L-1} basic wavelets of W_{L-1}:

$$
\left[\begin{array}{ccccc|cc|c}
0 & 0 & 6 & 0 & \frac{124}{35} & 0 & 0 & \\
0 & 0 & 0 & 0 & 1 & 0 & 0 & \\
0 & 0 & 0 & 0 & 0 & 0 & 1 & \ddots\\
\vdots & \vdots & \vdots & \vdots & 0 & 0 & 0 & \ddots\\
 & & & & \vdots & \vdots & \ddots & \ddots\\
\hline
1 & 0 & -\frac{418}{25} & 0 & -\frac{78973}{7875} & 0 & 0 & \\
0 & 1 & \frac{147}{25} & 0 & \frac{1327}{375} & 0 & 0 & \\
0 & 0 & \frac{4452}{25} & 1 & \frac{16094}{125} & 0 & 4 & \ddots\\
0 & 0 & 28 & 0 & \frac{658}{15} & 1 & 28 & \ddots\\
0 & 0 & 0 & 0 & 4 & 0 & 28 & \ddots\\
0 & 0 & 0 & 0 & 0 & 0 & 4 & \ddots\\
\vdots & \vdots & \vdots & \vdots & 0 & 0 & 0 & \ddots\\
 & & & & \vdots & \vdots & \ddots & \ddots
\end{array}\right].
$$

Here diagonal points mean that the preceding two columns are repeated the appropriate number of times while going each time two positions right and moving one position down. The last six columns of both blocks of the matrix R^L mirror the first six columns; the empty positions of matrices are equal to zero.

As a result, the values of the spline coefficients on the thinned grid and the wavelet coefficients are calculated by the formulas (7). Thus, the operation of wavelet decomposition can be performed without explicit representation and the use of a filter block.

The mathematical complexity of the algorithm for solving system (12) by the sweeping method is valued by the number of required arithmetic operations [27, p. 100]: $11\cdot(2^{L-1}-1)$ additions, $11\cdot(2^{L-1}-1)$ multiplications, and $2\cdot(2^{L-1}-1)+1$ divisions.

Calculating the right-hand sides of the equations requires $2 \cdot (2^{L-1} - 2)$ additions; obtaining the spline-coefficients at the nodes of the sparse grid requires 2 additions and 4 multiplications. The calculation of the wavelet-coefficients: $4 \cdot (2^{L-1} - 4) + 16$ multiplications and $4 \cdot (2^{L-1} - 4) + 14$ additions. If we make no differences between the arithmetic operations, then the total number of such operations for one step of the wavelet decomposition is approximately $34 \cdot 2^{L-1}$.

6 The algorithm of wavelet analysis

consists of performing the following steps:

6.1 On the finite segment $[a, b]$

the values of the observation results are reset to zero at the ends by subtracting values of the fifth degree Hermitian polynomial [20]

$$\sum_{i=0}^{2} (b-a)^i \left[f^{(i)}(a)\varphi_i(1-v) + f^{(i)}(b)\varphi_i(v) \right], \quad (13)$$

$$v = \frac{x-a}{b-a},$$

where

$$\varphi_i(t) = \begin{cases} t^3(6t^2 - 15t + 10), & i = 0, \\ -t^3(3t^2 - 7t + 4), & i = 1, \\ \dfrac{t^3}{2}(t^2 - 2t + 1), & i = 2, \end{cases}$$

from the entire time series.

6.2 The wavelet interpolation algorithm

for a given L is incorporated.

6.3 If $L > 3$,

then the value of L decreases by 1, and the algorithm goes to step 2.

6.4 Otherwise, at each level L

of the decomposition, the rejection of insignificant wavelet coefficients is performed according to some criterion [8, 21], and the spline coefficients are sequentially restored according to the moving average algorithm (4).

6.5 After wavelet analysis

of the differences obtained at the first stage of the algorithm and reconstructing (of course, with some approximation) the spline coefficients for the densest mesh, the values of the polynomial (13) are added to values of the approximating spline of the seventh degree.

7 Numerical experiments

7.1 Checking accuracy on polynomials

For $x \in [0, 1]$, assuming $L = 4$ at the upper resolution level, we find the grid step length $2^{-4} = 1/16$. When performing the wavelet transform, the values of the function at the nodes of the grid Δ^L are used as initial data, assuming zero values of the function and the derivatives at the ends of the segment, a total of 13 numbers.

Because the seventh-degree polynomial with eight zero boundary conditions does not exist we will bound considering the nine-degree polynomial $f(x) = x^4(x-1)^4(2x-1)$ as a test function. We find at the last stage of the recursive wavelet decomposition algorithm, four values of the boundary coefficients of the spline $S^3(x)$ at the ends of the segment, $C^3 = [-9.483 \cdot 10^{-6}, -7.916 \cdot 10^{-6}, 0, 7.916 \cdot 10^{-6}, 9.483 \cdot 10^{-6}]^T$. In this case, the wavelet coefficients are equal to $D^3 = [-8.275 \cdot 10^{-6}, 2.712 \cdot 10^{-7}, -2.779 \cdot 10^{-5}, 3.064 \cdot 10^{-5}, -3.064 \cdot 10^{-5}, 2.779 \cdot 10^{-5}, -2.712 \cdot 10^{-7}, 8.275 \cdot 10^{-6}]^T$. To demonstrate the accuracy property of the approximation scheme for polynomials of the ninth degree, we will neglect all the wavelet coefficients, providing a compression factor of 13/4=3.25, and we will show here the graph of the difference between the approximation spline and polynomial (Fig. 7), which has the alternating character from the ends of the interval.

7.2 The compression

coefficient in the considered example is small (only 8 wavelet coefficients are discarded). However, with an increase in the length of the smoothness intervals, the compression quality will undoubtedly be higher.

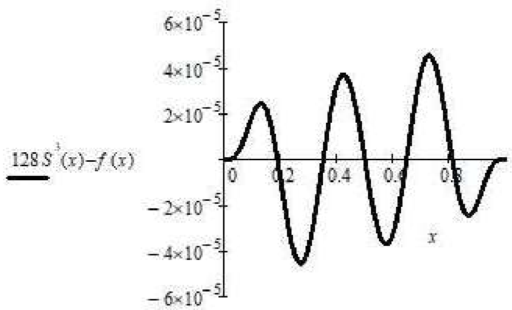

Figure 7: Graph of difference between the 7th-degree approximation spline and the nine-degree polynomial

8 Conclusion

The article discusses the further development of the author's procedure [22] for an even-odd partition of the defining system of the Hermite wavelet expansion for the practically important case of approximating that do not require specifying the values of the derivatives of the functions, based on B-splines of the seventh degree.

The advantage of the new algorithm is its simplicity of realization because of a matrix possessing five diagonals is solved at each step of decomposition.

The directions of our future research consist in the extension of the proposed approach to obtaining the seven-diagonal splitting method, possessing strict diagonal dominance, and to splines of a higher degree and of a larger number of zero moments which can provide new opportunities for the development of algorithms for performing wavelet-based signal de- and re-composition for Cartesian components of the geodata from laser scanning devices that issued in the form of the array ("cloud") of points, in which there is no division into separate cross scans.

References:

[1] W. Boehler, A. Marbs, 3D Scanning Instruments, *Proc. of the CIPA WG6 Int. 2002.* Workshop on scanning for cultural heritage recording. http://www.isprs.org/commission5/workshop/

[2] H. C. Yun, M. G. Kim, J. S. Lee, Applicability Estimation of Mobile Mapping System for Road Management, *Contemporary Engineering Sciences*, Vol.7, 2014, pp. 1407-1414.

[3] B.M. Shumilov, A.N. Baigulov, A study on modeling of road pavements based on laser scanned data and a novel type of approximating hermite wavelets, *WSEAS Transactions on Signal Processing*. Vol.11, 2015, pp. 150-156.

[4] C. De Boor, *A Practical Guide to Splines*, Applied Mathematical Sciences, Vol.27, Springer-Verlag, New York, 1978.

[5] J. D. Boissonnat, O. Devillers, M. Teillaud, M. Yvinec, Triangulations in CGAL, *Proc. 16th Annu. ACM Sympos. Comput. Geom.*, 2000, pp. 11-18.

[6] I. Daubechies, *Ten lectures on Wavelets*, Society for Industrial and Applied Mathematics, Philadelphia (PA), 1992.

[7] S. Mallat, *A Wavelet Tour of Signal Processing*, Academic Press, San Diego (CA), 1999.

[8] E.J. Stollnitz, T.D. DeRose, D.H. Salesin, *Wavelets for Computer Graphics*, Morgan Kaufmann Publishers, San Francisco, 1996.

[9] C.K. Chui, *An Introduction to Wavelets*, Academic Press, New York, London, 1992.

[10] M.F. Pouyani, M. Vali, M.A. Ghasemi, Lung sound signal denoising using discrete wavelet transform and artificial neural network, *Biomedical Signal Processing and Control*, Vol.72, 2022, article No. 103329

[11] M. Luo, L. Ge, Z. Xue, J. Zhang, Y. Li, X. Xiao, Research on De-noising of downhole engineering parameters by wavelet based on improved threshold function, *International Journal of Circuits, Systems and Signal Processing*, Vol.15, 2021, pp. 722-729.

[12] R. Wilson, Multiresolution image modeling, *Electronics and Communications Engineering Journal*, Vol.9, No.2, 1997, pp. 90-96.

[13] X. Li, S. Zhang, H. Zhao, A fast image compression algorithm based on wavelet transform, *International Journal of Circuits, Systems and Signal Processing*, Vol.15, 2021, pp. 809-819.

[14] Q. Zhang, Y. Li, Medical image segmentation algorithm based on multi-scale color wavelet texture, *International Journal of Circuits, Systems and Signal Processing*, Vol.15, 2021, pp. 928-935.

[15] P. Vonghirandecha, P. Bhurayanontachai, S. Kansomkeat, S. Intajag, No-reference retinal image sharpness metric using daubechies wavelet transform, *International Journal of Circuits, Systems and Signal Processing*, Vol.15, 2021, pp. 1064-1071.

[16] T. Tuncer, S. Dogan, P. Plawiak, A. Subasi, A novel Discrete Wavelet-Concatenated Mesh Tree and ternary chess pattern based ECG signal recognition method, *Biomedical Signal Processing and Control*, Vol.72, 2022, article No. 103331.

[17] A. Cohen, I. Daubechies, J.C. Feauveau, Biorthogonal bases of compactly supported wavelets, *Communications on Pure and Applied Mathematics*, Vol.45, 1992, pp. 485-560.

[18] A. Cohen, I. Doubeshies, P. Vial, Wavelets on the interval and fast wavelet transforms, *Applied and Computational Harmonic Analysis*, Vol.1, 1993, pp. 54-81.

[19] H. Demirel, G. Anbarjafari, Image resolution enhancement by using discrete and stationary wavelet decomposition, *IEEE Transactions on Image Processing*, Vol. 20, No. 5, pp. 1458-1460.

[20] V. Strela, Multiwavelets: regularity, orthogonality and symmetry via two-scale similarity transform. *Stud. Appl. Math.*, Vol.98, No.4, 1997, pp. 335-354.

[21] B.M. Shumilov, Multiwavelets of the third-degree Hermitian splines orthogonal to cubic polynomials, *Mathematical Models and Computer Simulations*, Vol.5, No.6, 2013, pp. 511-519.

[22] B.M. Shumilov, A splitting algorithm for wavelet transforms of the Hermite splines of the seventh degree, *Numerical Analysis and Applications*, Vol.8, No.4, 2015, pp. 365-377.

[23] F. Aràndiga, A. Baeza, R. Donat, Discrete multiresolution based on hermite interpolation: computing derivatives, *Communications in Nonlinear Science and Numerical Simulation*, Vol.9, 2004, pp. 263-273.

[24] B.M. Shumilov, Construction of an effective preconditioner for the even-odd splitting of cubic spline wavelets, *WSEAS Transactions on Mathematics*, Vol.20, 2021, pp. 718-728.

[25] K. Koro, K. Abe, Non-orthogonal spline wavelets for boundary element analysis, *Engineering Analysis with Boundary Elements*, Vol.25, 2001, pp. 149-164.

[26] S. Pissanetzky, *Sparse Matrix Technology*, Academic Press, London, 1984.

[27] A.A. Samarskii, E.S. Nikolaev, *Numerical Methods for Grid Equations, Vol. I Direct Methods*, Birkhauser, Basel, 1989.